

## Detection of stator winding fault in induction motor using instantaneous power signature analysis

Ahmet KÜÇÜKER\*, Mehmet BAYRAK

Department of Electrical-Electronics Engineering, Faculty of Engineering, Sakarya University, Sakarya, Turkey

Received: 09.04.2013

Accepted/Published Online: 17.06.2013

Printed: 28.08.2015

**Abstract:** Stator interturn faults are one of the most common faults occurring in induction motors. Early detection of interturn short circuit is important to reduce repair costs. Axial leakage monitoring, zero-sequence components, negative sequence current, and motor current signature analysis have been used for fault detection in early states. In the paper, the instantaneous power signature analysis technique is used to detect these faults, and experimental results for healthy and faulty motors are shown and discussed.

**Key words:** Fault detection, instantaneous power signature analysis, stator winding faults, induction motors

### 1. Introduction

Induction motors are a major irreplaceable part of industry and have an important role in the processes and production lines in many areas of industry. Hence, unexpected failures in these motors may create major problems. The Institute of Electrical and Electronics Engineers (IEEE) and the Electric Power Research Institute (EPRI) have done authoritative studies on this issue. The percentage of failures by component are given in Figure 1. Stator faults have 26% rates according to IEEE and 41% rates according to EPRI [1–3]. Sudden failures generally occur due to internal and external motor faults. The essential internal faults can broadly be classified as follows [4]:

- Stator winding faults,
- Rotor bar faults,
- Bearing faults,
- Mechanical imbalances.

Stator faults are caused by a combination of thermal, electrical, mechanical, and environmental stresses. One of the thermal stresses is thermal aging. An increase in temperature accelerates the aging process and thus reduces the lifetime of the stator windings. Another thermal stress is thermal overloading, which depends on unbalanced phase voltages, overloading, or ambient temperature. Mechanical stresses include coil movement and strikes from the rotor, bearing failures, shaft deflection, and eccentricity problems [5]. High humidity, aggressive chemicals, radiation from nuclear plants, or the salt level in seashore applications can be defined as

\*Correspondence: [kucuker@sakarya.edu.tr](mailto:kucuker@sakarya.edu.tr)

environmental stress. Electrical stresses include the negative influence of transient voltage conditions; turn-to-turn or turn-to-ground failures; line-to-line, line-to-ground, or multiphase line-to-ground faults in the supply; current limiting fuses; opening and closing of the circuit breakers; capacitor switching; or lightning strike [5].

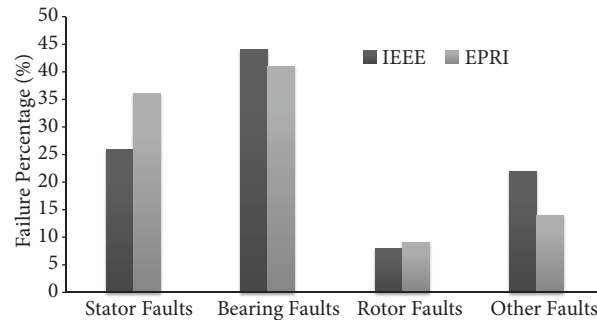


**Figure 1.** Percentage of failure by component.

In recent years, researchers have developed many techniques for detection of stator winding faults. Some protection algorithms include artificial neural network and wavelet-based stator fault detection methods in generators [6,7]. The third harmonic component has been used as an indication for turn-to-turn insulation failure faults with axial magnetic flux monitoring [8]. Zero-sequence components seen because of asymmetries in the machine impedances caused by stator winding faults have been reported [9]. In another work, a negative sequence component was detected because of stator winding fault in induction motor. However, even small supply voltage imbalances or load variations can produce large values of negative sequence currents. The effects of voltage unbalance and load variations must be compensated for by shorted-turn fault detection [10]. Ellipticity increasing with the severity of the stator fault associated with the faulty phase corresponding to the motor current Park's vector technique has been represented [11]. The continuous wavelet transform based on the Park's vector approach was used in another study. The frequency component at twice the supply frequency can be seen with Park's current vector [12].

Observation of the residual saturation harmonics technique, which is an offline technique, has been used to diagnose stator faults by measuring the odd multiples of the third harmonic in the induction motor terminal voltage right after switch-off [13].

The instantaneous currents space phasor (ICSP) approach has been proposed for stator winding fault detection. ICSP modulus ripple amplitudes and angular speed ripple amplitudes were recommended as a detection tool for online short circuits [14].

Motor current signature analysis is a commonly used technique based on frequency analysis. Some researchers have studied this technique, which was generally based on the observation of the main frequency side band [15]. However, some previous studies pointed that the spectrum method cannot show the side band clearly for detecting stator phase current signals used as input data. It also has limitations for identifying the level of fault severity [16,17]. Thus, this paper proposes the instantaneous power signature analysis (IPSA) technique for stator fault detection. The proposed method has an advantage for separating stator fault conditions from unbalanced voltage effects. The experiments carried out in this study using an induction motor under fault conditions show a significant increase in the characteristic components of the instantaneous power under both incipient and severe faults.

## 2. The proposed detection method

This paper proposes the use of instantaneous power analysis for detection of stator winding faults in induction motors. The IPSA method is examined at various motor load levels. During the implementation of this method, voltages and currents are necessary for implementing the instantaneous power signature. Suppose that an induction motor is energized by an ideal three-phase voltage.  $v(t)$  is the voltage between any two phases and  $i(t)$  is the current of these phases; these are given by Eqs. (1) and (2):

$$v(t) = U_m \cos(2\pi f_s t), \quad (1)$$

$$i(t) = I_m \cos(2\pi f_s t - \phi), \quad (2)$$

where  $U_m$  is the maximum value of the supply line to line voltage,  $I_m$  is the maximum value of the supply current,  $f_s$  is the supply frequency, and  $\phi$  is the initial phase angle of the supply current.

Partial instantaneous power  $p_0(t)$  can be written with Eqs (3) and (4).

$$p_0(t) = v(t).i(t) \quad (3)$$

$$p_0(t) = \frac{\sqrt{3}}{2} U_m I_m [\cos(2\pi(2f)t - \phi) + \cos(\phi)] \quad (4)$$

The total instantaneous power of a healthy induction motor can be calculated by Eq. (5) using the three-phase measured instantaneous voltages and currents.

$$p_{tot} = v_1(t)i_1(t) + v_2(t)i_2(t) + v_3(t)i_3(t) \quad (5)$$

The effects of stator faults cause characteristic side band currents in the current spectrum.  $f_{scf}$ , the frequency component, is a function of the short circuit and is given by Eq. (6) [18]:

$$f_{scf} = f_s \left( k \pm \frac{n}{p/2}(1-s) \right), \quad (6)$$

where  $f_r$  is the rotational frequency,  $f_s$  is the supply frequency,  $s$  is the slip,  $p$  is the number of poles, and  $n$  and  $k$  are two parameters ( $n = 1, 2, 3, \dots$ ,  $k = 1, 3, 5, \dots$ ).

Rotational frequency  $f_r$  can be defined as:

$$f_r = \frac{1-s}{p/2} f_s. \quad (7)$$

If a stator winding short circuit faults takes place in induction motor, fault characteristic components at  $f_{scf,i}$  appear in the stator current as given by Eq. (8) [18,19].

$$f_{scf,i} = k.f_s \pm n.f_r \quad (8)$$

$f_{scfp}$  is the right side band frequency and  $f_{scfn}$  is the left side band frequency, as shown in Eqs. (9) and (10).

$$f_{scfp} = k.f_s + n.f_r \quad (9)$$

$$f_{scfn} = k.f_s - n.f_r \quad (10)$$

$f_{scf,p}$  is the fault characteristic component in the power spectrum and can be defined as:

$$f_{scf,p} = 2.k.f_s \pm n.f_r \tag{11}$$

Stator winding short circuited induction motor current  $i_{scf}$  can be expressed as:

$$i_{scf}(t) = \left\{ \begin{array}{l} I_m \cos [2\pi f t - \theta] + \\ \sum_{k=1}^{\infty} \left\{ \begin{array}{l} I_{scfp} \cos [2\pi f_{scfp} t - \alpha_{scfp}] + \\ I_{scfn} \cos [2\pi f_{scfn} t - \alpha_{scfn}] \end{array} \right\} \end{array} \right\} \tag{12}$$

where  $I_{scfp}$  is the maximum value of the component at a frequency of  $(k.f_s + n.f_r)$ ,  $I_{scfn}$  is the maximum value of the component at a frequency of  $(k.f_s - n.f_r)$ ,  $\alpha_{scfp}$  is the phase angle of the component at a frequency of  $(k.f_s + n.f_r)$ , and  $\alpha_{scfn}$  is the maximum value of the component at a frequency of  $(k.f_s - n.f_r)$ .

The equation for the partial instantaneous power in the case of stator winding short circuit fault is given by Eq. (13) [18,20]. It can be seen that the instantaneous power spectrum contains an additional component at the modulation frequency.

$$p(t) = \left\{ \begin{array}{l} \frac{\sqrt{3}}{2} U_{m1} I_{m1} [\cos [2(2\pi f)t - \phi] + \cos \phi] + \\ \sum_{n=1}^{\infty} \left\{ \begin{array}{l} U_{m1} I_{scfn} \left[ \begin{array}{l} \cos \left[ \left( \frac{2k(2\pi f_s) -}{n(2\pi f_r)} \right) t - \phi_{scfn} \right] \\ + \cos [n(2\pi f_r)t + \phi_{scfn}] \end{array} \right] \\ + U_{m1} I_{scfp} \left[ \begin{array}{l} \cos \left[ \left( \frac{2k(2\pi f_s) +}{n(2\pi f_r)} \right) t - \phi_{scfp} \right] \\ + \cos [n(2\pi f_r)t - \phi_{scfp}] \end{array} \right] \end{array} \right\} \end{array} \right\} \tag{13}$$

### 3. Experimental results

Experimental studies were performed on a 3 kW, 220/380 V, 4 pole squirrel cage induction motor. Figure 2 shows the implemented test bench. Detailed parameters of the motor used in the experiments are given in the Appendix (on the journal’s website). A mechanical load is provided by a DC generator feeding a variable resistor. DC excitation current and load resistors are controllable. To emulate the fault conditions, the stator windings of the induction motor have been reconstructed. Thus, experiments have been done under different loading conditions.

In all experiments the stators are windings star connected and when a short circuit fault is introduced a shorting resistor is used to limit the short circuit current, thus protecting the stator windings from complete failure. Figure 3 illustrates the scheme of the experimental system to detect faulty conditions.

The data were acquired using LabVIEW software. Test results were obtained under healthy, winding short circuit and phase-to-phase short circuit conditions, which can be seen in Figure 4. Stator winding at 10% short circuit fault for one phase, and 10% to 10% for phase-to-phase short circuit have been tested.

For a four-pole induction motor operating at a frequency of 50 Hz under no-load condition, the instantaneous power has 75 Hz, 125 Hz, 175 Hz, and 225 Hz frequencies for the stator fault condition obtained from Eq. (11) where  $k = 1$  and  $k = 2$ .

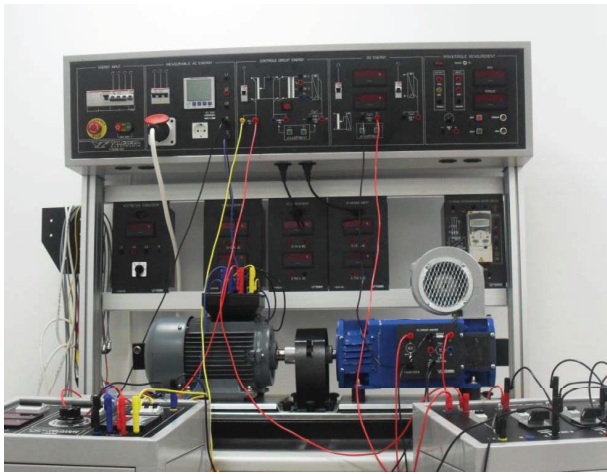


Figure 2. Experimental test bench.

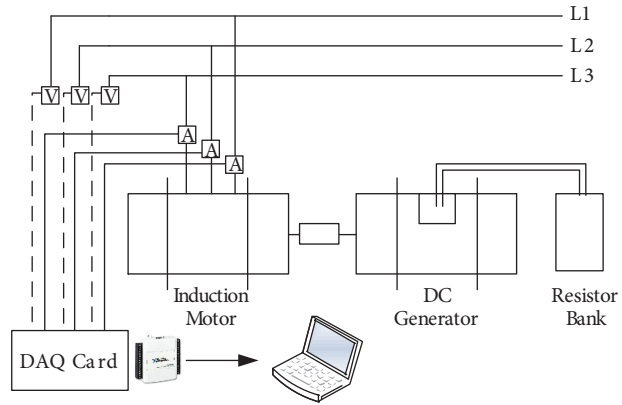


Figure 3. Detection system scheme.

IPSA of a healthy motor is shown in Figure 5. Increase of the stator fault frequencies can be clearly seen for the two types of stator faults. Stator interturn winding short circuit fault and phase-to-phase short circuit faults are clearly detected with no-load conditions. This can be clearly seen from Figures 6 and 7.

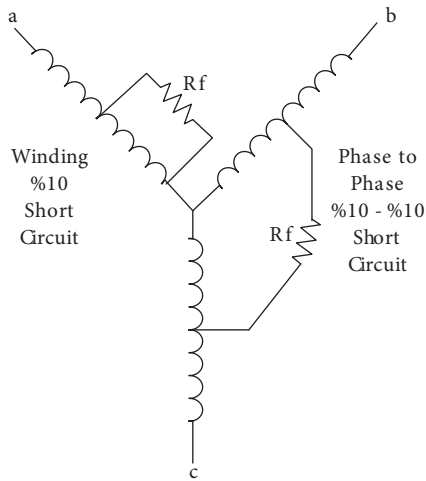


Figure 4. Stator short circuit faults.

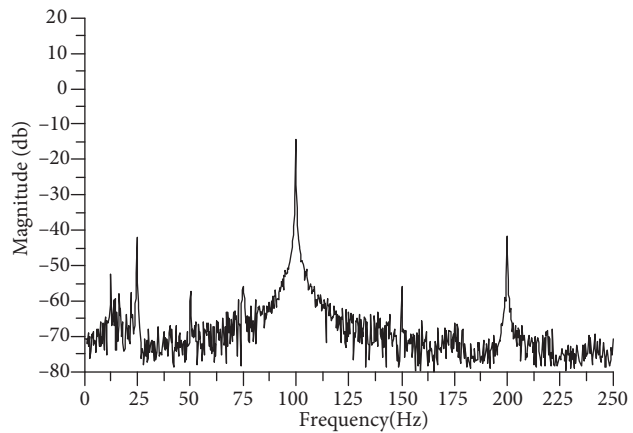


Figure 5. Healthy-condition IPSA with no load.

In addition, different load levels were analyzed in the laboratory tests. Healthy motor IPSA with 50% load is shown in Figure 8. Figure 9 shows stator winding short circuit IPSA with 50% loading and Figure 10 shows the stator winding phase-to-phase short circuit IPSA with 50% loading.

Side band frequencies reflected to the instantaneous power stator fault frequencies were clearly detected. Healthy motor IPSA, stator winding short circuit IPSA, and stator winding phase-to-phase short circuit IPSA with 100% loading are shown in Figures 11–13, respectively.

Under loading conditions, the instantaneous power has 75.5 Hz, 124.5 Hz, 175.5 Hz, and 224.5 Hz frequency components for the stator short circuit fault obtained from Eq. (11) where  $k = 1$  and  $k = 2$  and  $s = 0.02$ .

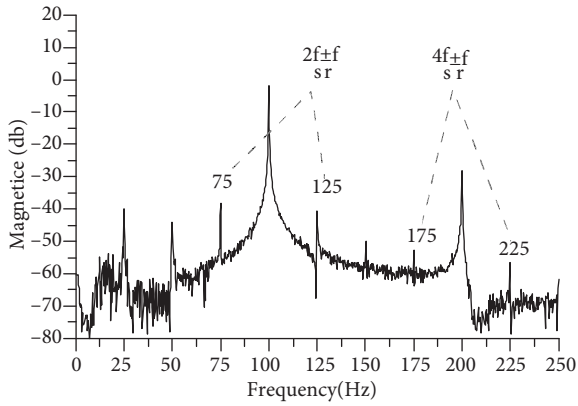


Figure 6. Stator winding short circuit IPSA with no load.

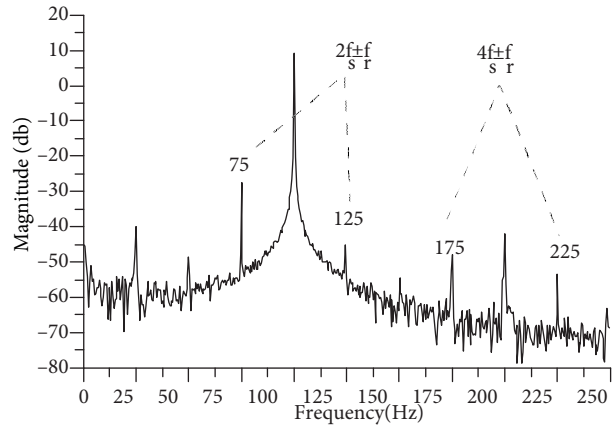


Figure 7. Stator winding P-P short circuit IPSA with no load.

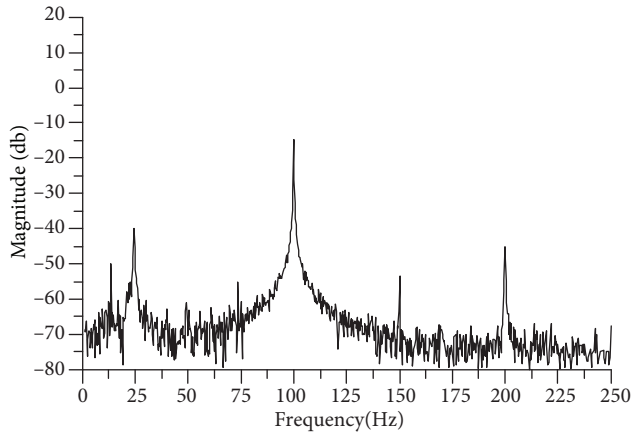


Figure 8. Healthy-condition IPSA with 50% loading.

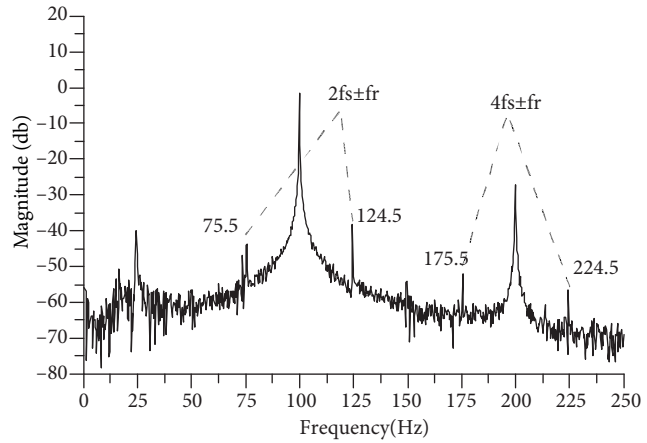


Figure 9. Stator winding short circuit IPSA with 50% loading.

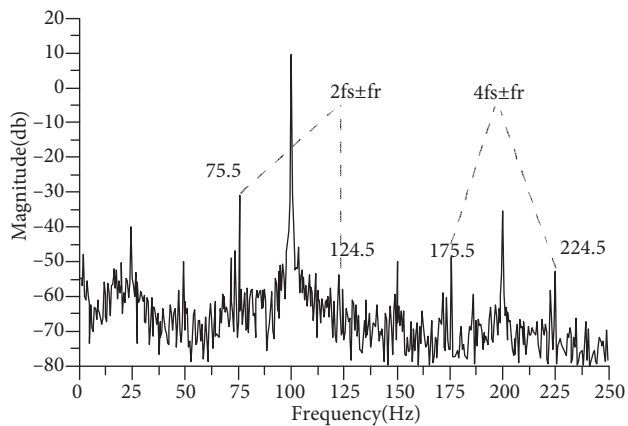


Figure 10. Stator winding P-P short circuit IPSA with 50% loading.

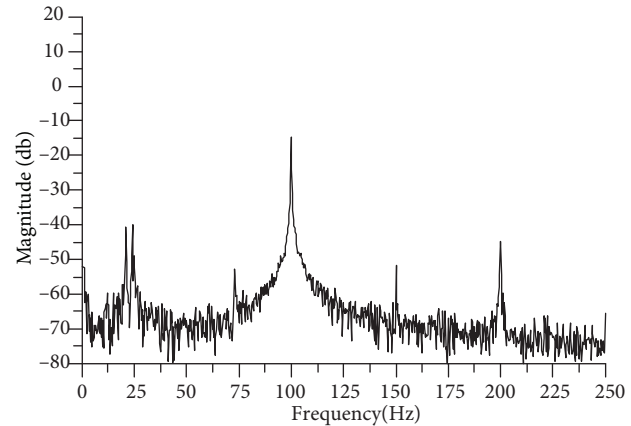
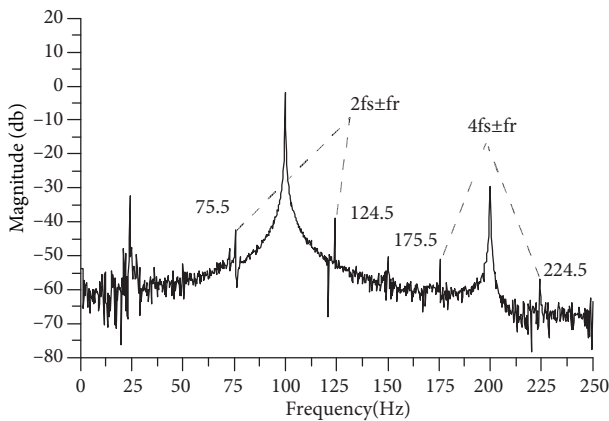
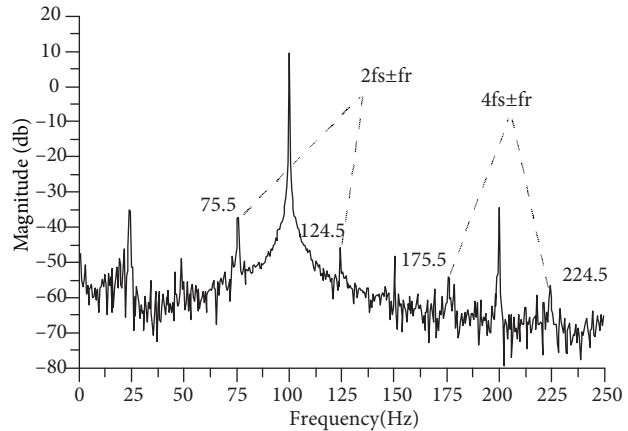


Figure 11. Healthy condition IPSA with 100% loading.



**Figure 12.** Stator winding short circuit IPSA with 100% loading.



**Figure 13.** Stator winding P-P short circuit IPSA with 100% loading.

The Table gives the results of IPSA and magnitudes of the frequency components for healthy condition, stator interturn short circuits, and stator phase-to-phase short circuit conditions. An increase at 100 Hz frequency can be seen, besides the  $f_{scf,p}$  frequencies. However, this increase may have occurred because of unbalanced voltages. Therefore, frequencies detected with IPSA will be important in the detection of stator faults.

**Table.** IPSA significant frequency components.

	No load		Under 50% load		Under 100% load	
	$F_{comp}$ Hz	Mag. db	$F_{comp}$ Hz	Mag. db	$F_{com}$ Hz	Mag. db
Healthy condition	25	1-37	25	2-34	25	3-32
	75	4-48	75	5-60	75	6-65
	100	7-14	100	8-14	100	9-14
	125	10-63	125	-65	125	11-63
	175	12-66	175	13-80	175	-67
	225	14-86	225	15-72	225	16-72
Stator interturn short circuit	25	17-27	24.5	18-32	24.5	19-32
	75	20-38	75.5	21-43	75.5	22-42
	100	23-2	100	24-1	100	25-2
	125	26-40	124.5	72-38	124.5	28-39
	175	29-52	175.5	30-56	175.5	31-56
	225	32-56	224.5	33-56	224.5	34-58
Stator phase-to-phase short circuit	25	-34	24.5	35-32	24.5	36-35
	75	37-27	75.5	-30	75.5	38-37
	100	9	100	9.5	100	9.5
	125	39-49	124.5	40-58	124.5	41-48
	175	42-48	175.5	43-48	175.5	44-54
	225	45-53	224.5	46-53	224.5	47-58

#### 4. Conclusion

The effectiveness of the proposed method is shown by laboratory experiments on a three-phase induction motor. The theoretical considerations have been validated by experimental results.

Results have shown that stator short circuit faults in an induction motor could be detected using simple and low-cost techniques that utilize the instantaneous power measurements. The presence of stator short circuit faults was detected by the increase in the specific fault frequencies in instantaneous power measurements. Phase-to-phase short circuit fault frequency magnitudes were more distinguishable than stator winding interturn short circuit fault frequency magnitudes.

In other respects, the use of instantaneous power provides information about the current and voltage values, which may be important when unbalanced voltage, voltage sags, and other abnormal electrical faults occurred.

## Appendix

Parameters of motor used in the experiments.

Rated power 3 kW

Rated voltage 220 V

Rated current 6.45 A

Rated frequency 50 Hz

Rated speed 1405 r/min

Number of poles 4

Stator connection wye

$I_A/I_N$  5.0

$M_A/M_N$  2.4

J 0.005 kgm<sup>2</sup>

## References

- [1] IAS Motor Reliability Working Group. Report of large motor reliability survey of industrial and commercial installations, Part I. IEEE T Ind Appl 1985; 21: 853–864.
- [2] IAS Motor Reliability Working Group. Report of large motor reliability survey of industrial and commercial installations, Part II. IEEE T Ind Appl 1985; 21: 865–872.
- [3] IAS Motor Reliability Working Group. Report of large motor reliability survey of industrial and commercial installations, Part III. IEEE T Ind Appl 1987; 23: 153–158.
- [4] Bayrak M, Küçük A. Detection of rotor bar corrosion in three phase asynchronous motors using wavelet analysis. In: MEPS 2010 Modern Electric Power Systems Proceedings of the International Symposium; 20-22 September 2010; Wrocław, Poland. pp. 1–5.
- [5] Grubic S, Aller JM, Lu B, Habetler TG. A survey on testing and monitoring methods for stator insulation systems of low-voltage induction machines focusing on turn insulation problems. IEEE T Ind Electron 2008; 55: 4127–4136.
- [6] Khan A, Ozgonenel O, Rahman MA. Wavelet transform based protection of stator faults in synchronous generators. Electr Pow Compo Sys 2007, 35: 625–637.
- [7] Özgönenel Ö, Yalçın T. A complete motor protection algorithm based on PCA and ANN: a real time study. Turk J Electr Eng Co 2011, 19: 317–334.
- [8] Toni K, Slobodan M, Aleksandar B. Detection of turn to turn faults in stator winding with axial magnetic flux in induction motors. In: IEEE Electric Machines & Drives Conference; 3–5 May 2007; Antalya, Turkey. New York, NY, USA: IEEE. pp. 826–829.
- [9] Briz F, Degner MW, Garcia P, Diciz AB. Induction machine diagnostics using zero sequence component. In: IEEE Industry Applications Conference; 2–6 October 2005; Kowloon, Hong Kong. New York, NY, USA: IEEE. pp. 34–41.



- [10] Bakhri S, Ertugrul N, Soong WL, Arkan M. Investigation of negative sequence components for stator shorted turn detection in induction motors. In: 20th Australasian Universities Power Engineering Conference; 5–8 December 2010; Christchurch, New Zealand. pp. 1–6.
- [11] Cardoso AJM, Cruz SMA, Fonseca DSB. Inter-turn stator winding fault diagnosis in three-phase induction motors, by park's vector approach. *IEEE T Energy Conver* 1999; 14: 595–598.
- [12] Spyropoulos DV, Mitronikas ED. Induction motor stator fault diagnosis technique using Park vector approach and complex wavelets. In: 2012 XXth International Conference on Electrical Machines; 2–5 September 2012; Marseille, France. pp. 1730–1734.
- [13] Nandi S. Detection of stator faults in induction machines using residual saturation harmonics. *IEEE T Ind Appl* 2006; 42: 1201–1208.
- [14] Crăciunescu A, Ciumbulea G, Media M. Stator winding fault diagnostic of induction motor using instantaneous currents' space phasor approach. *Prz Elektrotechniczn* 2012; 88: 108–111.
- [15] Thomson WT. On-line MCSA to diagnose shorted turns in low voltage stator windings of 3-phase induction motors prior to failure. In: *IEEE International Electric Machines and Drives Conference*; 17–20 July 2001; Cambridge, MA, USA. New York, NY, USA: IEEE. pp. 891–898.
- [16] Zagirnyak M, Mamchur D, Kalinov A. Comparison of induction motor diagnostic methods based on spectra analysis of current and instantaneous power signals. *Prz Elektrotechniczn* 2012; 88: 221–224.
- [17] Treetrong J. Fault detection of electric motors based on frequency and time-frequency analysis using extended DFT. *Int J Control Autom* 2011; 4: 49–58.
- [18] Gandhi A, Corrigan T, Parsa L. Recent advances in modeling and online detection of stator interturn faults in electrical motors. *IEEE T Ind Electron* 2011; 58: 1564–1575.
- [19] Legowski SF, Sadrul Ula AHM, Trzynadlowski AM. Instantaneous power as a medium for the signature analysis of induction motors. *IEEE T Ind Appl* 1996; 32: 904–909.
- [20] Zhenxing L, Xianggen Y, Zhe Z, Deshu C, Wei C. Online rotor mixed fault diagnosis way based on spectrum analysis of instantaneous power in squirrel cage induction motors. *IEEE T Energy Conver* 2004; 19: 485–490.